SIMULATION OF A FIBER PUSHOUT TEST IN A MODEL POLYESTER/EPOXY COMPOSITE

Philippe H. Geubelle [1,2], Guoyu Lin [2] and Nancy R. Sottos [3]

[1] *Aeronautical and Astronautical Engineering, University of Illinois*
[2] *Center for the Simulation of Advanced Rockets, University of Illinois*
[3] *Theoretical and Applied Mechanics, University of Illinois*
Talbot Laboratories; 104 South Wright Street; Urbana, IL 61801; USA

SUMMARY: We present a detailed simulation of the fiber pushout process observed in a model composite system. The finite element scheme used in the analysis combines conventional "volumetric" elements to represent the mechanical response of the fiber and the surrounding matrix, and cohesive elements introduced along the fiber/matrix interface and used to capture the spontaneous frictional debonding process. An augmented Lagrangian scheme is used to capture the frictional contact taking place behind the spontaneously propagating crack tip between the newly created crack faces. Comparison between numerical and experimental results obtained for a polyester fiber/epoxy matrix composite system shows excellent agreement. We then present a parametric study of the effects on the energetics and stability of the failure process of quantities such as the frictional interface strength and the fiber/matrix stiffness mismatch.

KEYWORDS: fiber pushout and pullout, cohesive fracture, frictional debonding, cohesive finite element, interface.

INTRODUCTION

Fiber pullout and pushout tests performed on model composite systems involving a single macro-fiber embedded in a polymeric, metallic or ceramic matrix (Fig. 1) are now routinely used to extract interface properties such as fracture toughness and friction coefficient [1-5]. These two interface properties are usually extracted from the evolution of the load applied on the fiber (P) and the resulting displacement of the pushout/pullout tool (Δ_p), and from observations of the propagation of the debonding front (L_c). A typical force-displacement curve obtained for a pushout test is schematically presented in Fig. 2, showing three distinct stages. After the specimen has settled on its support, one observes a linear response corresponding to perfect fiber/matrix bonding (stage I). Then, as the load increases, a crack initiates from the top of the specimen and propagates along the fiber/matrix interface, generating a nonlinear punch load/displacement curve (stage II). When the crack reaches a

critical value, the debonding process becomes unstable and leads to a sudden complete debonding of the fiber from the matrix. This is the onset of stage III which corresponds to the frictional sliding of the fiber out of the surrounding matrix.

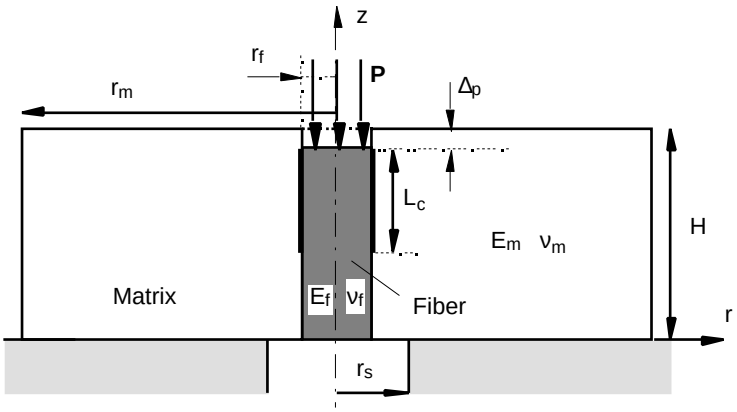

Fig. 1: Geometry of the fiber pushout test

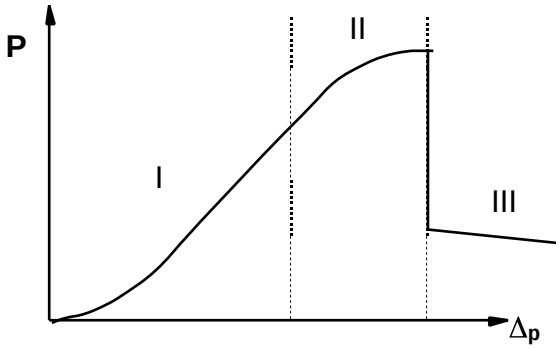

Fig. 2: Typical punch load versus displacement curve in a pushout test.

It should be noted however that, while the failure process described above is characteristic of many fiber pullout and pushout tests, some debonding and sliding events can be quite different. For example, bottom debonds are observed in model composite systems characterized by high stiffness mismatch between the fiber and the matrix [4]. In some situations, the frictional sliding is not uniform and continuous as eluded to earlier, but takes place in a dislocation-like fashion [3,6].

To support these experiments, various theoretical and numerical analyses have been performed. At the theoretical level, the shear lag method [7-9] provides in closed form a valuable insight on the effects of parameters such as the fiber length and radius, the friction coefficient, the modulus mismatch, etc. However, by neglecting surface and end effects, the shear lag method tends to over-predict the interface fracture toughness [4,10]. At the numerical level, various investigations have focused on the frictional sliding stage [11,12] and, in particular, on the importance of the friction model on the continuous/discontinuous character of the sliding process.

While the accurate capture of the frictional contact between the crack faces remains an important component in the present study, the emphasis of the work described hereafter is somewhat different. The basic objective of this project is to develop a cohesive-based finite element scheme able to capture the spontaneous initiation and propagation of an interface crack, including the presence of stress concentrations. In other words, we focus on the first two stages of the fiber pullout process.

After a brief overview of the numerical method, we present a detailed comparison between numerical results and the experimental observations obtained recently by Bechel and Sottos [4,10] on a model polyester/epoxy composite system. We then perform a parametric study of the effects on the failure process of some important parameters such as the fiber/matrix stiffness mismatch and the frictional strength of the interface.

DESCRIPTION OF THE NUMERICAL SCHEME

As described earlier, the numerical scheme adopted in this study is a special axisymmetric version of the cohesive/volumetric finite element (CVFE) scheme, which has been successfully used over the past few years in the simulation of a wide variety of quasi-static [13-15] and dynamic [16-18] fracture events.

Details on the derivation of the finite element formulation can be found in a related paper [19]. We limit our present description of the numerical scheme to a discussion of the cohesive failure model. In this study, we use a simple bilinear relation to express the cohesive traction vector $\boldsymbol{T}$ acting on the fiber/matrix interface in terms of the associated interfacial separation (or displacement jump) vector Δ. The cohesive model is shown in Fig. 3 for the purely shear (mode II) failure case. In Fig. 3, the tangential (T_t) cohesive traction is normalized by its respective critical values (τ_{max}). The tangential (Δ_t) displacement jump is also normalized by its critical values (Δ_t^c) defined as the value of the tangential displacement discontinuity (or slip) beyond which complete failure is achieved. Similar parameters denoted by σ_{max} and Δ_n^c are defined for purely tensile (mode I) cohesive failure. In the mixed-mode case, normal and tangential failures are coupled by expressing the normal and tangential components of the cohesive traction vector $\mathrm{T} = \left(T_n, T_t\right)$ in terms of the Euclidean norm of the displacement jump vector $\Delta = \left(\Delta_n, \Delta_t\right)$ [19].

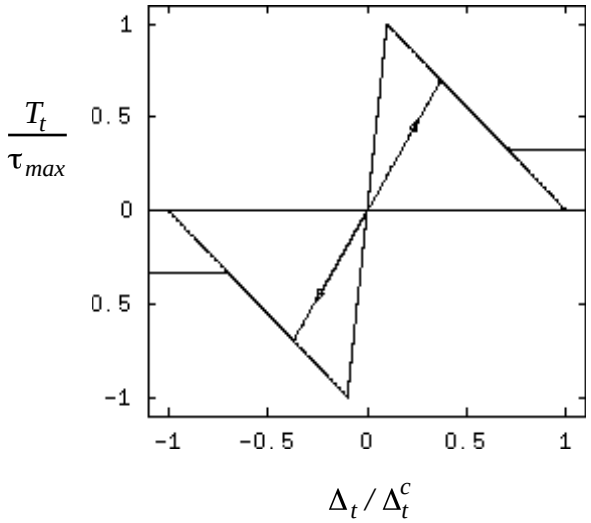

Fig. 3: Bilinear cohesive failure law for the pure mode II case ($\Delta_n = 0$). The solid and dashed curves correspond to frictional and frictionless contact, respectively. The arrows indicate the evolution of the shear cohesive traction in the event of unloading after partial failure.

The normal and tangential works of separation per unit area of interface, also referred to as mode I and mode II fracture toughnesses, are then given by

$$G_I^c = \sigma_{max}\Delta_n^c / 2\,; \qquad G_{II}^c = \tau_{max}\Delta_t^c / 2\,. \tag{1}$$

It has to be noted that this particular debonding failure process takes place almost exclusively under pure shear (mode II) conditions. Therefore, although present in the finite element formulation, the aforementioned coupling between normal and tangential modes does not play a major role in the analysis.

Finally, to account for the frictional contact between the crack faces behind the advancing crack front, a simple Coulomb friction model with constant friction coefficient μ is introduced. The augmented Lagrangian treatment [20] is used to constrain the frictional sliding along the debonded interface and to enforce the appropriate contact conditions. It should be noted that the contact detection method used in this work is only local in that contact is only enforced when occurring between initially adjacent elements. While this approach is obviously not sufficient to model the frictional sliding part of the pushout test (stage III) for which substantial relative sliding takes place, it is expected to be sufficient to capture the frictional debonding phase (stage II).

An illustration of the mesh used in the analysis is presented in Fig. 4. It is composed of 1024 four-noded volumetric elements and 104 four-noded cohesive elements evenly distributed along the fiber/matrix interface. The domain size is chosen to match those used in Bechel and Sottos' experiments [4]: fiber radius $r_f=0.95mm$, specimen radius $r_m=4.3mm$, specimen thickness $H=5.36mm$ and support inner radius $r_s=1.025mm$.

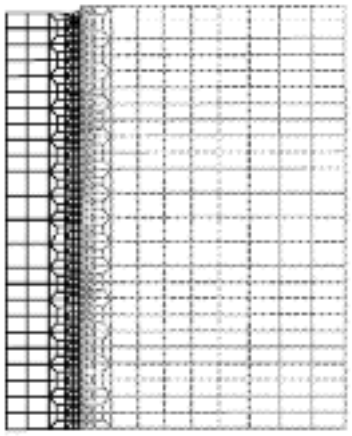

Fig.4: Finite element mesh (shown in its deformed shape) used in the fiber pushout study.

COMPARISON WITH EXPERIMENTAL RESULTS

In a series of very detailed experiments, Bechel and Sottos [4,10] investigated the mechanics of fiber pushout by simultaneously measuring the evolution with respect of the punch displacement of the punch load and of the crack tip location. The model composite system used in their study was made of a polyester fiber ($E_f=2.5GPa$ and $\nu_f=0.35$) and an epoxy matrix ($E_m=4GPa$ and $\nu_m=0.33$). They measured a chemical shrinkage strain $\varepsilon_{th}=-0.0022$ in the matrix, a friction coefficient $\mu=0.52$ and a mode II fracture toughness $G_{II}^c=0.11N/m$.

This leaves us with only one parameter τ_{max} to fully define the numerical model described in the previous section. Actually, two additional parameters (σ_{max} and G_I^c) are needed which define the normal cohesive failure. We have chosen to take $\sigma_{max}=\tau_{max}$ and $G_I^c=G_{II}^c$ for simplicity, noting, once again, that since the failure process takes place almost exclusively in shear, these two parameters hardly play any role in the simulation of the debonding event. This simulation constitutes an excellent test for the CVFE scheme since the choice of a single

fitting parameter τ_{max} must allow us to capture two independent measurements: the punch load vs. displacement curve *and* the crack tip location vs. punch displacement curve. As shown in Fig. 5, an excellent agreement between experimental and numerical results is achieved in both cases.

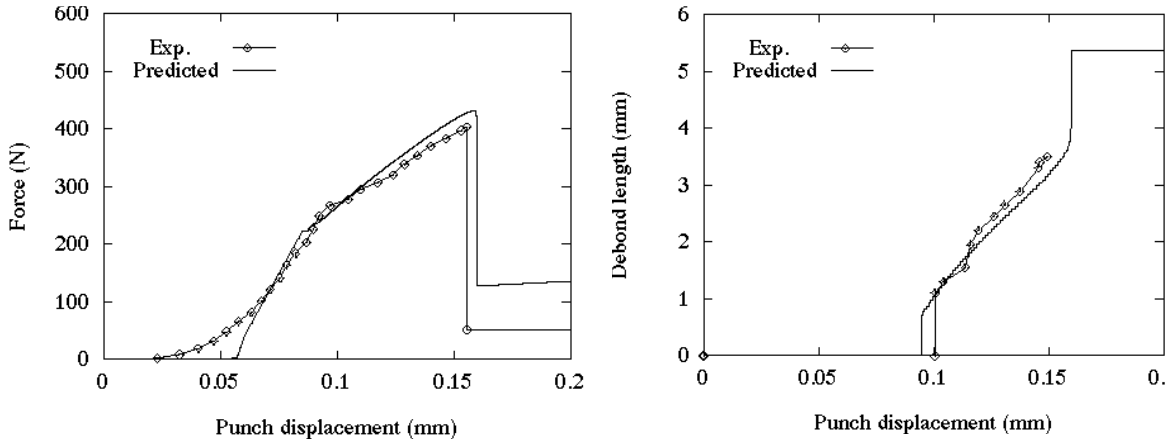

Fig. 5: Comparison between experimental and numerical results: punch load vs. displacement curve (left) and evolution of the crack tip location (right).

The corresponding value of the interface shear strength τ_{max} is $22N/mm^2$. By comparison, the value of the interface strength obtained by the usual "strength of materials" approach, i.e., by evenly distributing the maximum punch load over the entire fiber outer surface, is $12.5N/mm^2$. Note also how well the numerical scheme is able to capture the onset of the unstable crack growth precursor to the frictional sliding stage (stage III).

The numerical simulation allows us to readily compare the energy dissipated in the cohesive failure to that associated with the frictional contact between the crack faces. As apparent in Fig. 6, the frictional contact accounts for most of the energy dissipation.

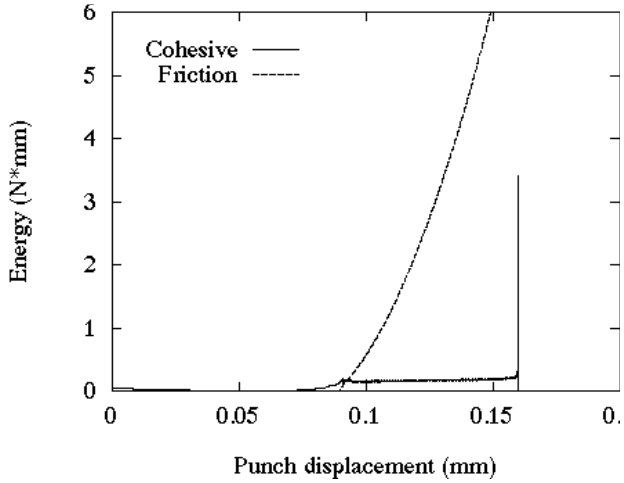

Fig. 6: Energetics of the debonding process, showing that frictional contact account for most of the energy dissipation.

Finally, Fig. 7 present the evolution of the shear and tensile traction stress acting on the interface for various values of the crack length. As apparent in Fig. 7, the stress concentration present in the vicinity of the advancing crack front is well captured by the CVFE scheme, together with that associated with the frictional contact in the vicinity of the top surface of the

specimen (*z=5.36mm*). As indicated earlier, these two strong stress concentrations are not accounted for in the shear lag analysis of the fiber pushout.

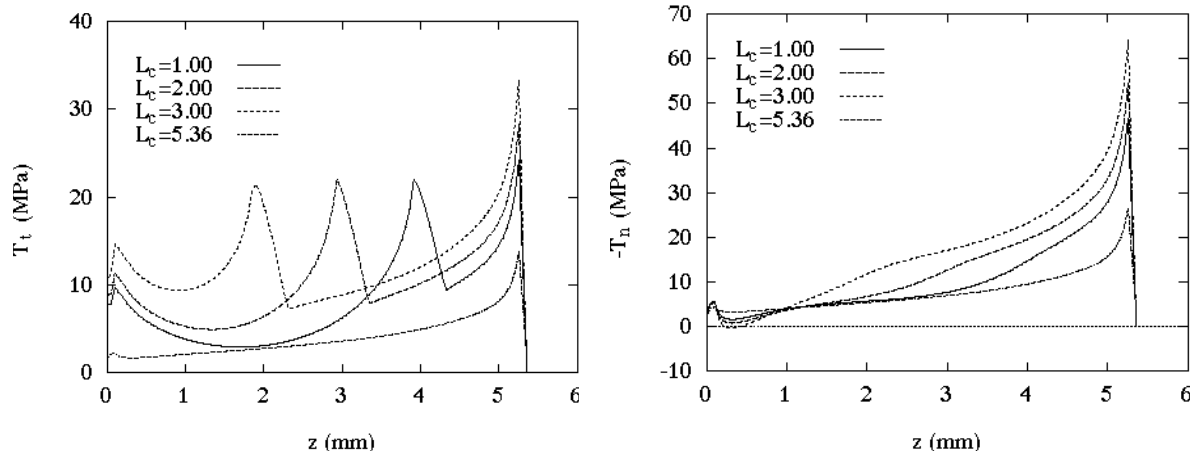

Fig. 7: Evolution of the shear (T_t) and normal (T_n) cohesive traction stress acting along the fiber/matrix interface at different stages of the debonding process. The crack length L_c is expressed in *mm* and is measured from the top of the sample (*z=5.36mm*).

PARAMETRIC STUDY

Having demonstrated the ability of the CVFE scheme to simulate the spontaneous debonding process, we now turn our attention to the investigation of the effects of various parameters on the mechanics of fiber pushout. Due to space constraints, we will limit our discussion in the present paper to just two parameters: the fiber/matrix stiffness mismatch and the frictional strength of the interface. Discussion of other parameters, such as the amplitude of the residual strains and the interface cohesive strength can be found in Ref. 19.

Effect of the fiber/matrix stiffness mismatch (E_f/E_m)

Experimental observations [4] indicate that the stiffness mismatch strongly affects the debonding process, especially with regards to the appearance of top vs. bottom debond. These observations are confirmed by the numerical results, which indicate that, as the stiffness ratio E_f/E_m increases, a transition takes place from a top (for $E_f/E_m<2$) to a bottom debond (for *Ef/Em>4*). For intermediate values of the stiffness ratio, both types of crack initiation are predicted. It should be also noted that all top debond cases involve quasi-exclusively mode II type of failure, as the crack faces are constantly in contact over their entire length. For the bottom debonding cases, some opening is observed and the failure process takes place under mixed mode conditions, especially in the early stages of the interface debonding process. However, prior to the complete debonding of the interface, contact takes place between the failure surfaces and the failure process is once again of purely mode II type.

A good way to characterize the transition between top and bottom debonds is through a map summarizing the combined effects of the residual strain and the modulus mismatch, such as that shown in Fig. 8. The trend presented there is very similar to the experimental map presented in Fig. 9 of [4]: as it is the case experimentally, the transition does not seem to depend much on the residual strain, but varies strongly with the stiffness ratio.

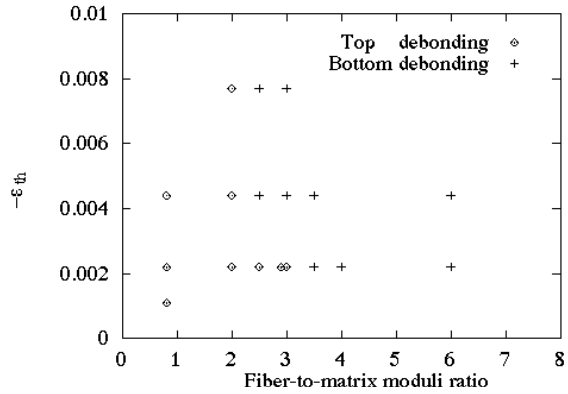

Fig. 8: Top vs. bottom debond map.

Effect of the friction coefficient (μ)

As alluded to in the previous section, friction between the crack faces plays a crucial role in the energetics of the overall failure process, especially for composite systems characterized by the presence of high compressive residual stresses acting on the fiber/matrix interface. As shown in Fig. 9, the friction coefficient also plays a very important role in the stability of the frictional debonding process: the load carrying capability of the fiber greatly increases with μ, thereby delaying the onset of the complete debond and the frictional sliding of the fiber out of the matrix.

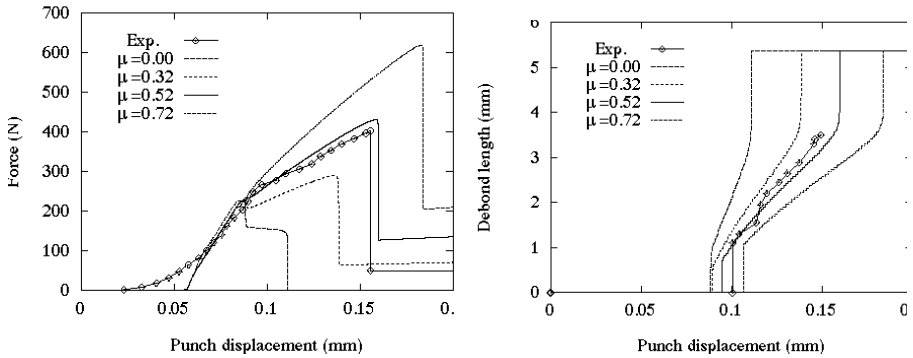

Fig. 9: Effect of the friction coefficient μ on the punch load vs. displacement curve (left) and on the evolution of the crack tip length (right) for a polyester/epoxy composite system.

CONCLUSIONS

We have presented a detailed simulation of quasi-static fiber pushout in a model polyester/epoxy composite system. The method used in this study is a special axisymmetric cohesive/volumetric finite element scheme which includes a augmented Lagrangian treatment of the frictional contact between the spontaneously created fracture surfaces. By introducing cohesive elements along the fiber/matrix interface, we are able to simulate the spontaneous initiation and propagation of the debonding crack front. The numerical simulations agree very well with experimental observations, with regards to the punch load vs. displacement curve, the evolution of the debond length and the onset of unstable crack growth. Numerical results indicate that frictional contact accounts for the most of the energy dissipation associated with

the debonding process. Parametric studies have also been performed to characterize the effects of the stiffness mismatch and of the friction coefficient on the initiation and propagation of the interfacial crack.

ACKNOWLEDGEMENTS

This work has been supported by the ASCI Center for the Simulation of Advanced Rockets located at the University of Illinois at Urbana and funded by the U.S. Department of Energy through the University of California under Subcontract number B341494.

REFERENCES

1. Bowling, J. and Grove, G.W., "The debonding and pull-out of ductile wires from a brittle matrix", *J. Mat. Sc.*, Vol. 14, 1979, pp. 431-442.

2. Atkinson, C., Avila, J., Betz, E. and Smelser, R.E., "The rod pull-out problem, theory and experiment", *J. Mech. Phys. Solids*, Vol. 30, No. 3, 1982, pp. 97-120.

3. Tsai, K.-H. and Kim, K.-S., "The micromechanics of fiber pull-out", *J. Mech. Phys. Solids*, Vol. 44, No. 7, 1996, pp. 1147-1177.

4. Bechel, V. and Sottos, N.R., "Application of debond length measurements to examine the mechanics of fiber pushout", *J. Mech. Phys. Solids*, Vol. 46, No. 9, 1998, pp. 1675-1697.

5. Khanna, S. K. and Shukla, A., "Influence of fiber inclination and interfacial conditions on fracture in composite materials", *Exper. Mech.*, Vol. 34, No. 2, 1994, pp. 171-180.

6. Kendall, K., "Model experiments illustrating fibre pull-out", *J. Mater. Sc.*, Vol. 10, 1975, pp. 1011-1014.

7. Shetty, D. K., "Shear-lag analysis of fiber push-out (indentation) tests for estimating interfacial friction stress in ceramic-matrix composites", *J. Am. Ceram. Soc.*, Vol. 71, No. 2, 1988, pp. C-107-109.

8. Hutchinson, J. W. and Jensen, H. M., "Models of fiber debonding and pullout in brittle composites with friction", *Mech. Mat.*, Vol. 9, 1990, pp. 139-163.

9. Liang, C. and Hutchinson, J. W., "Mechanics of the fiber pushout test", *Mech. Mat.*, Vol. 14, 1993, pp. 207-221.

10. Bechel, V. and Sottos, N. R., "A comparison of calculated and measured debond lengths from fiber pushout test", *Comp. Sc. Tech.*, Vol. 58, 1998, pp. 1727-1739.

11. Freund, L. B., "The axial force needed to slide a circular fiber along a hole in an elastic material and implications for fiber pull-out", *Eur. J. Mech. A/Solids*, Vol. 11, No. 1, 1991, pp. 1-19.

12. Povirk, G. L. and Needleman, A., "Finite element simulations of fiber pull-out", *J. Eng. Mater.*, Vol. 115, No. 3, 1993, pp. 286-291.

13. Needleman, A., "A continuum model for void nucleation by inclusion debonding", *J. Applied Mech.*, Vol. 54, 1987, pp. 525-531.

14. Lin, G., Kim, Y.-J., Cornec, A., and Schwalbe, K.-H., "Fracture toughness of a constrained metal layer", *Comp. Mat. Science*, Vol. 9, 1997, pp. 36-47.

15. Tvergaard, V. and Hutchinson, J. W., "The relation between crack growth resistance and fracture process parameters in elastic-plastic solids", *J. Mech. Phys. Solids*, Vol. 40, 1992, pp. 1377-1397.

16. Needleman, A., "Numerical modeling of crack growth under dynamic loading conditions", *Comp. Mech.*, Vol. 19, No. 6, 1997, pp. 463-469.

17. Camacho, G. T. and Ortiz, M., "Computational modelling of impact damage in brittle materials", *Int. J. Solids Structures*, Vol. 30, No. 20-22, 1996, pp. 2899-2938.

18. Geubelle, P. H. and Baylor, J., "Impact-induced delamination of composites: a 2D simulation", *Composites B*, Vol. 29B, 1998, pp. 589-602.

19. Lin, G., Geubelle, P. H. and Sottos, N. R., "Simulation of fiber debonding and frictional sliding in a model composite pushout test", Submitted to *Int. J. Solids & Structures*, 1998.

20. Simo, J. C. and Laursen, T. A., "An augmented Lagrangian treatment of contact problems involving friction", *Comp. & Struct.* , Vol. 42, No. 1, 1992, pp. 97-116.